



STUDY OF WETTABILITY OF DIFFERENT MILD STEEL SURFACES

Xuanping Tang, Sonja Richter and Srdjan Nestic
Institute for Corrosion and Multiphase Technology
Department of Chemical and Biomolecular Engineering
Ohio University
342 West State Street
Athens, OH 45701

ABSTRACT

Water wetting is a common phenomenon affected by, among other things, water chemistry, flow regime, pipe orientation and water cut. The nature of the wetted surface itself, such as bare metal surfaces with different degree of roughness or a surface covered with iron carbonate film, can affect wetting. In order to quantify the wettability of a steel surface by oil or water phase as well as to understand how surface conditions affect the wettability, contact angles measurements were performed using a novel goniometer system specially designed for this project. Contact angles of water-in-oil droplets and oil-in-water droplets on bare steel surfaces of different roughness and iron carbonate film covered surfaces were measured. It was found that water-in-oil contact angle changes with time. Iron carbonate film makes the surface more hydrophilic and water droplets wet the surface more quickly. For relatively smooth bare metal surfaces, surface roughness has no major effect on contact angle. For the oil-in-water contact angle measurements, the contact angle doesn't show time dependency and the nature of the steel surface has no effect on contact angle. Furthermore, in these tests the crude oil type did not affect oil-in-water contact angle.

Keywords: water wetting, goniometer, contact angle, wettability, roughness, crude oil, iron carbonate

INTRODUCTION

Crude oil and ground water with complex water chemistry are transported simultaneously in oil pipelines. Different oil-water flow patterns can exist, which lead to different distributions of oil and water phases in the cross-section of pipe. At low oil-water mixture velocity, the water phase can flow as a water layer on the bottom of pipe. However, at higher velocity, the water can be entrained by the oil phase and flow as droplets in the continuum of the oil phase. Corrosive gases such as CO₂ and H₂S

Copyright

©2009 by NACE International. Requests for permission to publish this manuscript in any form, in part or in whole must be in writing to NACE International, Copyright Division, 1440 South creek Drive, Houston, Texas 777084. The material presented and the views expressed in this paper are solely those of the author(s) and are not necessarily endorsed by the Association. Printed in the U.S.A.

Government work published by NACE International with permission of the author(s). The material presented and the views expressed in this paper are solely those of the author(s) and are not necessarily endorsed by the Association. Printed in the U.S.A.

dissolve in the water phase and create a more corrosive environment. In the field, most crude oil pipelines are made of carbon steel. Once corrosive water wets the inner pipe wall, corrosion can occur. The likelihood of corrosion generally increases with increasing the volume fraction of water. Other important factors which are important for water wetting and corrosion are: water chemistry, crude oil compositions, additives (corrosion/scaling inhibitor, drag reducing agent (DRA), etc.) and pipe wall surface state (scales, films, etc.).

During last three decades, the effects of these parameters on water wetting have been considered only in a qualitative sense. The first simplified water wetting model, which was used to predict the critical oil velocity needed to sweep out the settled water in the pipe, was proposed by Wicks and Fraser¹(1975). This model was only based on limited experimental results and was suitable for very low water cut situations. At high water cuts, the model significantly underestimated the critical velocity needed for entrainment. Simon Thomas et al.²(1987) pointed out that oils could entrain water up to a 20% water cut at oil velocities larger than 1 m/s. C. de Waard and Lotz³ (1993) argued that the presence of the hydrocarbon phase was accounted through a so-called oil factor. Based on the original experiments of Wicks and Fraser¹ a binary prediction factor was extracted suggesting that oil-wetting will occur only for water cuts less than 30% and oil velocity larger than 1 m/s. Adams et al.⁴(1993) pointed out that three types of phase wettings could occur and estimated that below 30% water cut the tubing will be oil-wet; from 30-50%, intermittent water wetting occurs, and over 50% the tubing is water wet. Obviously, these are very crude criteria that neglect or oversimplify the effects of varying properties of the oil and water phases and flow regime, etc. Furthermore, field experience suggests that in some cases corrosion was obtained at water cuts as low as 2%, in others no corrosion was obtained for water cuts larger than 50%. Wu⁵(1995) modified the Wicks and Fraser¹ model, however no major advancement was achieved. C. de Waard et al.⁶ updated their original empirical model³ and proposed a new empirical model using an analysis based on the emulsion breakpoint approach. A link between API gravity, emulsion stability and water wetting of steel by an oil-water mixture was considered by taking into account the changes of interfacial tensions in an oil-water-steel system. However, while agreeing reasonably well with the specific pool of field cases used for its calibration, this new model remains an empirical correlation built on limited field data with an uncertain potential for extrapolation. More importantly, this model does not consider the effects of internal pipe wall surface state, pipe diameter, oil density, oil viscosity and system temperature on the critical velocity of the flowing oil phase required for entrainment.

A mechanistic model (Cai et al.⁸ and Nesic et al.⁹, 2004) of water wetting prediction in oil/water and gas/oil/water systems is included in a software package MULTICORP released from Ohio University. This model follows Brauner¹⁰ and Barnea¹¹ for prediction of water-in-oil fully dispersed flow deriving a criterion for forming stable water-in-oil dispersed flow by means of calculating the critical velocity for water entrainment. The effects of pipe diameter, pipe inclination, oil density, oil viscosity and system temperature on the critical velocity of the flowing oil phase required for entrainment are considered in the model. It should be pointed out that the model has not been verified in gas-oil-water three-phase flow and does not consider the effects of gas, steel surface state, chemical additives and type of crude oil on water wetting because of lack of experimental and field data.

In 2005, a comprehensively experimental campaign, along with numerical modeling of water wetting in large diameter oil-water two-phase flows, was carried out at the Institute for Corrosion and Multiphase Technology of Ohio University^{12,13,14}. Comprehensive phase wetting maps for different oils have been built at different pipe inclinations in oil-water two-phase flows. The effects of oil type and pipe inclination on phase wetting and CO₂ corrosion have been extensively investigated. However, it should be addressed that the effects of surface conditions on water wetting and CO₂ corrosion have not been considered in that experimental campaign. The research was carried out with relatively smooth

pipe surface, i.e. bare metal surface. In order to understand the effect of pipe surface state on water wetting and CO₂ corrosion and further update current water wetting model by considering this effect, a new project was initialized. It is expected that the effect of metal surface state will be captured by the modification of the friction factor and interfacial tension in the current model. As a part of work on this project, a series of experiments were conducted to investigate the effect of steel surface state on wettability.

Wetting, in general, is the interaction of a liquid phase with a solid phase when surrounded by a gas phase or a second liquid phase. There are many common examples of wetting phenomena, such as the spreading of a liquid over a surface, the penetration of a liquid into a porous medium, or the displacement of one liquid by another. The interfaces which are produced can be solid/liquid, solid/gas or solid/liquid, liquid/gas or liquid/liquid. Wettability is most often described by the geometry of a sessile or resting drop. Contact angle (θ) is a measure of wettability and is defined as the angle between the surfaces of the liquid and the solid substrate at the line of contact, as measured from the side of the liquid. A schematic diagram of contact angle is shown in Figure 1. A low contact angle means high wettability or hydrophilia and a high contact angle means poor wettability or hydrophobia¹⁶.

The contact angle between two phases is controlled by the molecular interaction between the phases. At the interface, the molecules of each phase interact with each other resulting in an interfacial force, which is called adhesion force. Meanwhile, the particles within the same phase interact among themselves, producing intrafacial force, which is called cohesion force. The result of this competition of forces results in an interfacial tension γ . The strength of the interfacial tension $\gamma_{s/g}$ and $\gamma_{s/l}$ is a measure of the interfacial energy of the correspondent interfaces. The interfacial energy can be defined¹⁷:

$$\gamma_{ij} = \left(\frac{\delta F}{\delta A_{ij}} \right)_{T,V,n(K)} \quad (1)$$

Where γ_{ij} : interfacial energy at the interface between the phase i and j,

F : Helmholtz free energy,

A_{ij} : surface area between phases i and j,

T : absolute temperature,

V : volume,

$n(K)$: the number of surface excess moles of the component k.

The different interfacial tensions reach equilibrium when the free energy of the system is minimum, and this produces the shape of the liquid interface which is primarily defined by the contact angle (Figure 1). In thermodynamic equilibrium the contact angle θ in Figure 1 is given by Young's equation¹⁸.

$$\gamma_{s/g} - \gamma_{s/l} = \gamma_{l/g} \cos \theta \quad (2)$$

Where $\gamma_{s/g}$: interfacial energy at the interface between solid and gas phase,

$\gamma_{s/l}$: interfacial energy at the interface between solid and liquid phase,

$\gamma_{l/g}$: interfacial energy at the interface between liquid and gas phase.

Although there are many commercial instruments available, they are generally based on the sessile droplet method or the Wilhelmy plate method with gas as one of the phases. Therefore a novel

goniometer system based on the sessile droplet method has been designed and built to determine contact angles of oil-in-water or water-in-oil droplets on the metal surface.

EXPERIMENTAL PROCEDURE

There are two main instrumentations used in this research. One is a goniometer for contact angle measurements and the other is a glass cell in which, iron carbonate film covered surface is created.

The goniometer consists of two main parts, the test cell and image capture system as shown in Figure 2. The test cell is a 4" O.D., 3 3/4" I.D and 6" height transparent cylindrical tube made of polycarbonate and is shown in Figure 3. There are two 2" circular openings made in the opposite sides on the tube wall to accommodate flat windows that will avoid the distortion of the droplet image. A carbon steel test piece is mounted on a Teflon mount inside the cell. There are two entry ports on the cell wall for injecting water droplet (in an oil environment) on top of the test piece or oil droplet (in a water environment) on the metal test piece. The metal test piece is made of X65 mild steel and its dimension is shown in Figure 4. Only one circular side of the test piece is used as test surface and all other sides are coated with Teflon. On the bottom of the cell wall, two access ports in are made for liquid drainage and infusion. The image capture system is composed of a camera, a backlight, a PCI card and image analysis software. The camera used is monochrome CCD camera with 768 x 494 pixel array, 570 horizontal lines of resolution. The PCI card installed in the computer connects to the camera to get the image of droplet displayed on the computer screen. Using the image analysis software one can calculate contact angles from the captured images.

Water-in-oil contact angle measurement was conducted with four different surface conditions as seen in Table 1, which consist of bare metal surface with three different surface roughnesses of 1.5 μm , 6 μm and 40 μm and iron carbonate film covered surface with a roughness of 20 μm . 1.5 μm , 6 μm roughness bare metal surfaces are achieved by using 400 and 36 grit SiC paper, respectively. 40 μm roughness surface is created by machine scratching. Infinite Focus Microscope (IFM) is used for surface roughness characterization. Figure 5 shows the IFM images for the surfaces with different roughness. The test liquids are LVT200 model oil and 1 wt% NaCl brine. A droplet volume of 5~8 μl was used in the current research.

In order to develop iron carbonate film on the carbon steel test piece, a glass cell is deployed, which setup is show in Figure 6. The iron carbonate film covered surface is produced in 1 wt% NaCl brine under an environment of pH of 6.6 and temperature of 80 °C. Bare metal surface with roughness of 40 μm was hung in the cell and exposed to these conditions for 24 hours. The Scanning Electron Microscope (SEM) is used to verify the formation of iron carbonate film. The SEM images for the iron carbonate film covered surface before and after the contact angle test are shown in Figure 7 and Figure 8. By comparing these two figures, it can be found that the iron carbonate film covered surface does not change during the contact angle test. The test matrix for the formation of iron carbonate film is shown in Table 2.

The test matrix for the oil-in-water contact angle measurements in Table 3 is similar to that for water-in-oil contact angle measurement except that 6 different oils are used to create oil droplets. The main properties for the oils, such as density, dynamic viscosity, surface tension and interfacial tension, are shown Figure 9 in -Figure 12. C5 is the heaviest oil while C1 is the lightest one. Accordingly, C5 has the biggest dynamic viscosity while C5 is the least viscous oil. All oils have very similar surface tension.

The oil-water interfacial tension of 5 crudes is smaller than that of LVT200, which means these 5 crudes are easier to mix with water.

The test cell set up for introducing water droplets on metal surface is shown in Figure 13. With a microliter syringe a drop of liquid can be positioned on the surface of the metal plate for instance a water droplet in oil phase (sessile droplet). A droplet of oil can be released from a microliter syringe into the water phase as shown in Figure 14 and then the drop floats to a position under the steel test piece.

The following test procedure for sessile droplet was used:

1. Put the test coupon in the coupon holder and the continuous liquid into the cell,
2. Purge the test cell with CO₂ and deoxygenate for more than half an hour,
3. Inject droplet on the surface of the carbon steel test piece through the injection port.
4. Capture the image of the droplet on the surface of the test piece.
5. Measure the contact angle between the droplet and the surface of the test piece.
6. Injecting a new droplet on a new position of the coupon surface and repeat from 1 – 5.

EXPERIMENTAL RESULTS

Water-in-oil contact angle

The evolution of the contact between the water droplet and the steel surface is a dynamic process. The effects of time on contact angle for different surface conditions can be seen in Figure 15. In first 5 seconds, the contact angle decrease from the initial 180° .

The effect of the surface roughness on the contact angle can be deduced from Figure 16. The contact angles for 1.5 μm, 6 μm and iron carbonate covered surface are all around 40°, which is smaller than the contact angle of 70° for 40 μm surface. That means 1.5 μm, 6 μm and iron carbonate covered surface are more hydrophilic than the 40 μm surface. It can be concluded that for the relatively smooth bare metal surfaces, the surface roughness has no major effect on the contact angle, which is much smaller than the contact angle of the roughest surfaces. Iron carbonate film makes the surface more hydrophilic.

Oil-in-water contact angle

The contact angles of oil droplets on steel surfaces exposed to 1 wt% NaCl brine are measured and the results are shown in Figure 17. The contact angles for different oil phases are approximately the same, which are all around 150°, especially for the crude oils. Figure 18 shows the typical images of different oil droplets on 6 μm steels surface. The crude oil type does not affect the oil-in-water contact angle. In Figure 17, it also can be seen that the contact angles for each kind of oil droplet on different surfaces are approximately the same. This is not surprising since all the oils tested had approximately similar physico-chemical properties. The surface roughness or state does not affect the contact angle. All oil-in-water contact angles are around 150°, which validates that the steel surfaces of different roughness are all hydrophilic.

From Young's equation (Equation 2), it can be deducted that water-in-oil contact angle and oil-in-water contact angle are complementary for the same oil and the same water phase. From Figure 19 it can

be seen that the sums of oil-in-water and water-in-oil contact angles for 1.5 μm , 6 μm surface and iron carbonate covered surface are around 200° , which is rather close to the theoretical 180° . But for the roughest 40 μm surface, the sum is about 230° , which indicates a larger hysteresis in contact angle for the roughest steel surface. Contact angle hysteresis is caused by the existence of many thermodynamic metastable states for systems having three-phase boundaries, such as surface heterogeneity and surface roughness.

CONCLUSIONS

A comprehensive experimental research study has been carried out to investigate the effect of steel surface state on the phase wettability. The major points can be concluded as following.

For water-in-oil contact angle measurement,

- Contact angle changes with time before the contact between liquid droplet and solid surface reaches equilibrium state,
- Iron carbonate film makes the surface more hydrophilic,
- For the relatively smooth bare metal surfaces, the surface roughness has no major effect on the contact angle, which is much smaller than the contact angle of the rougher surfaces.

For oil-in-water contact angle measurement,

- The oil-in-water contact angle does not show a time dependency,
- The state of the steel surface has no major effect on the oil-in-water contact angle,
- Furthermore, various crude oil types tested currently did not affect the oil-in-water contact angle.

ACKNOWLEDGEMENT

Financial supports from BP, ConocoPhillips, ENI, ExxonMobil, Petrobras, Saudi Aramco, Shell and Total for the Institute for Corrosion and Multiphase Technology of Ohio University are gratefully acknowledged.

REFERENCES

- 1 Wicks, M., and Fraser, J.P., "Entrainment of Water By Flowing Oil", Materials Performance, May 1975, pp. 9~12.
- 2 M.J.J. Simon Thomas, C. de Waard and L.M.Smith "Controlling Factors in the Rate of CO_2 Corrosion", UK. Corr.'87 Brighton, 26-28 Oct., 1987
- 3 C. de Waard and U. Lotz, "Prediction of CO_2 Corrosion of Carbon Steel", Corrosion/93, paper no. 69, (Houston, TX: NACE International, 1993)
- 4 C. D. Adams, J. D. Garber, F. H. Walters, C. Singh, "Verification of Computer Modeled Tubing Life Predictions by Field Data", Corrosion/93, paper no. 82, (Houston, TX: NACE International, 1993)
- 5 Wu, Y., "Entrainment Method Enhanced to Account for Oil's Water Content", Oil & Gas Technology, Aug. 28, 1995, pp. 83~86.

- 6 C.de Waard, L.Smith and B.D. Craig, "The Influent of Crude Oil on Well Tubing Corrosion Rates", EUROCORR 2001.
- 7 S. Nestic, Jiyong Cai, Shihuai Wang, Ying Xiao and Dong Liu, Ohio University Multiphase Flow and Corrosion Prediction Software Package MULTICORP V3.0, Ohio University(2004).
- 8 Jiyong Cai, Srdjan Nestic and Cornelis de Waard, "Modeling of Water Wetting in Oil-Water Pipe Flow", NACE 2004, Paper No.04663, pp. 1-19, 2004.
- 9 Srdjan Nestic, Jiyong Cai and Kun-Lin John Lee, "A Multiphase Flow and Internal Corrosion Prediction Model for Mild Steel Pipelines", NACE 2005, Paper No.05556.
- 10 Brauner, N., "The Prediction of Dispersed Flows Boundaries in Liquid-Liquid and Gas-liquid Systems", *Int. J. of Multiphase Flow*, Vol.27, pp. 885~910(2001)
- 11 Barnea, D., "A Unified Model for Predicting Flow Pattern Transitions for the Whole Range of Pipe Inclinations", *Int. J. of Multiphase Flow*, Vol.11, pp. 1~12(1987).
- 12 Li C., Tang X., Ayello F., Cai J., Nešić S., "Experimental Study on Water Wetting and CO₂ Corrosion in Oil-Water Two-Phase Flow", NACE CORROSION/06, Paper No. 06595, San Diego, CA, 2006
- 13 Tang X., "Effects of Oil Type on Phase Wetting Transition and Corrosion in Oil-water Flow", NACE CORROSION/07, Student Poster Session, Nashville, TN, 2007
- 14 Ayello F.; Li C. Tang X.; Nešić S.; "Determination of phase wetting in oil-water pipe flows"; NACE CORROSION/08, Paper No. 08566, New Orleans, LA, 2008
- 15 Jiyong Cai, Srdjan Nestic, Chong Li, Xuanping Tang, Francois Ayello, C. Ivan T. Cruz and Jamal N. Khamis, "Experimental Studies of Water Wetting in Large Diameter Horizontal Oil-Water Pipe Flows", SPE 2005, Paper No. 95512-PP.
- 16 John C. Berg, "Wettability", M. Dekker, Inc., New York, 1993
- 17 G. Schmitt, "Wettability of steel surfaces at CO₂ corrosion conditions I. effect of surface active compounds in aqueous and hydrocarbon media", CORROSION'98, NACE International, Houston/TX, paper No.28
- 18 T. Young, Phil, Trans, 95: 65, 82 (1805)
- 19 Drelich, Changpeng Fang and C. L. Measurement of Interfacial Tension in Fluid-Fluid Systems White In Encyclopedia of Surface and Colloid Science Marcel Dekker, Inc., New York 2003, pp. 3152-3166

7. APPENDIX

Table 1 Test matrix for water-in-oil contact angle measurement

Steel type	Carbon steel X65
Surface conditions	Bare metal surface: <ul style="list-style-type: none"> • 1.5 μm (#400 sand paper) • 6 μm (#36 sand paper) • 40 μm (machined) iron carbonate film covered surface: <ul style="list-style-type: none"> • 20 μm
Temperature	25 °C
Oil phase	LVT200
Water phase	1 wt% NaCl brine
Droplet volume	2.5 μl , 5 μl and 10 μl
pH	4.0
CO ₂ partial pressure	0.96 bar
Deoxygenation time	Half an hour for oil phase in cell, more than one hour for water phase

Table 2 Test matrix for iron carbonate film formation

Steel type	Carbon steel X65
Original surface conditions	machined surface with 40 μm roughness
Temperature	80 °C
CO ₂ partial pressure	0.52 bar
pH	6.6
Time	24 hrs
Temperature	80 °C

Table 3 Test matrix for oil-in-water contact angle measurement

Steel type	Carbon steel X65
Surface conditions	Bare metal surface: <ul style="list-style-type: none"> • 1.5 μm (#400 sand paper) • 6 μm (#36 sand paper) • 40 μm (machined) iron carbonate film covered surface: <ul style="list-style-type: none"> • 20 μm
Temperature	25°C
Oil phase	LVT200, C1, C2, C3, C4, C5
Water phase	1 wt% NaCl brine
pH	4.0
CO ₂ partial pressure	0.96 bar
Deoxygenation time	One hour for water phase in cell, half an hour for oil phase

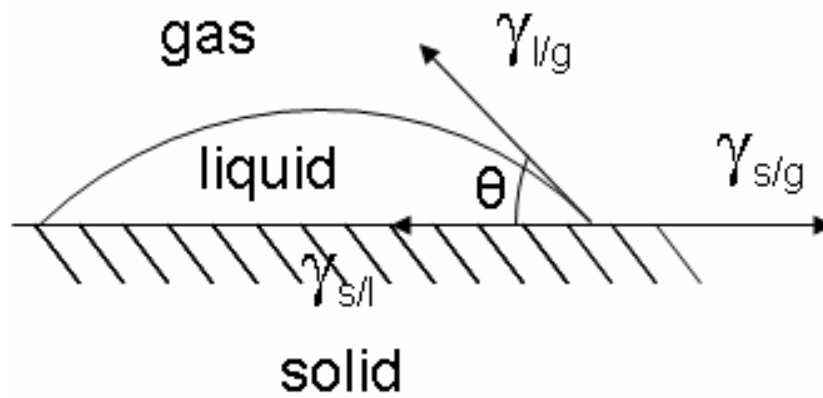


Figure 1 Schematic of contact angle

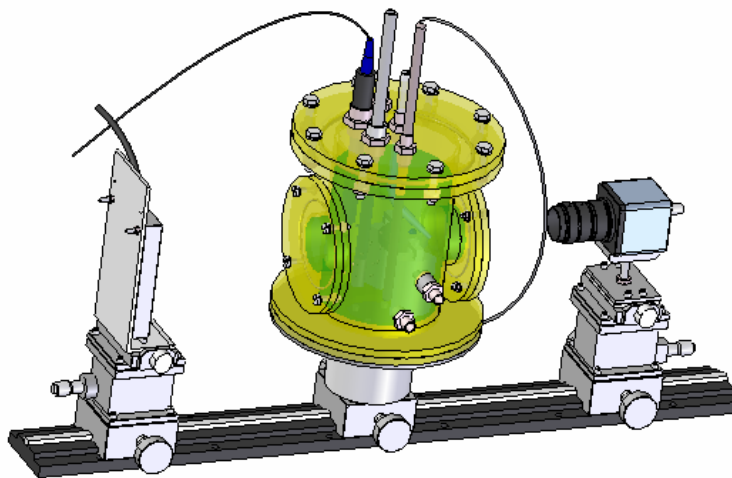


Figure 2 Goniometer with optical imaging camera and backlight

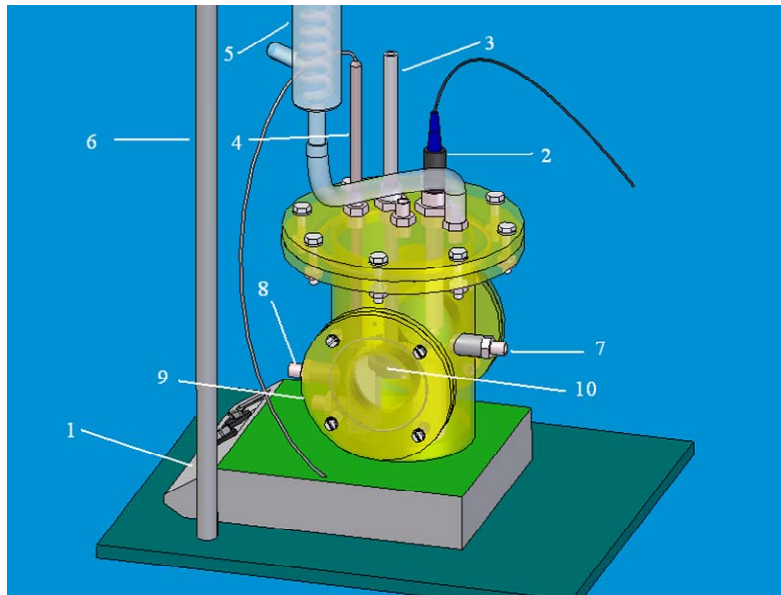


Figure 3 Full view of test cell (1. Heat plate 2. pH probe 3. CO₂ bubbler 4. Temperature probe 5. Condenser 6. Condenser holder 7. Water droplet injector 8. Oil droplet injector 9. Drainage 10. Test piece)

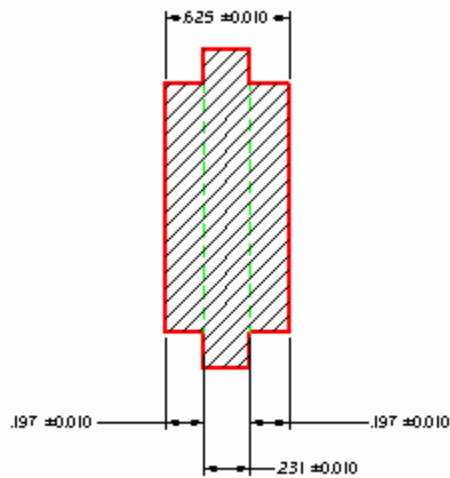


Figure 4 Dimension of carbon steel test piece (Unit: Inch)

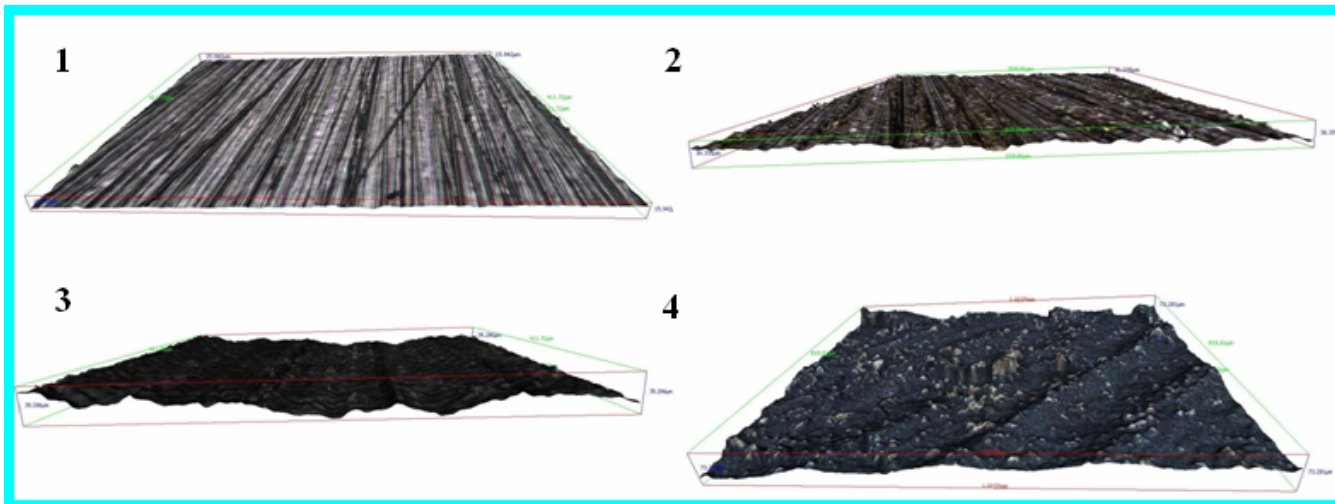


Figure 5 IFM images for surfaces with different roughness
(1, 2, 3 stand for 1.5, 6, and 40 μm roughness bare metal surface, respectively.
4 stands for iron carbonate surface with 20 μm roughness)

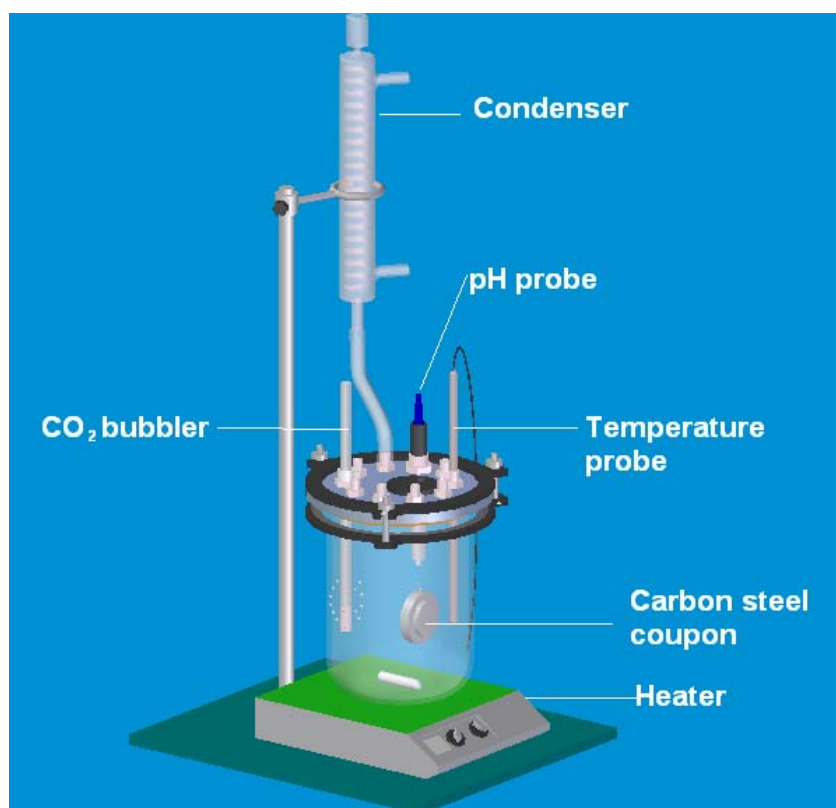


Figure 6 Glass set up for iron carbonate film formation

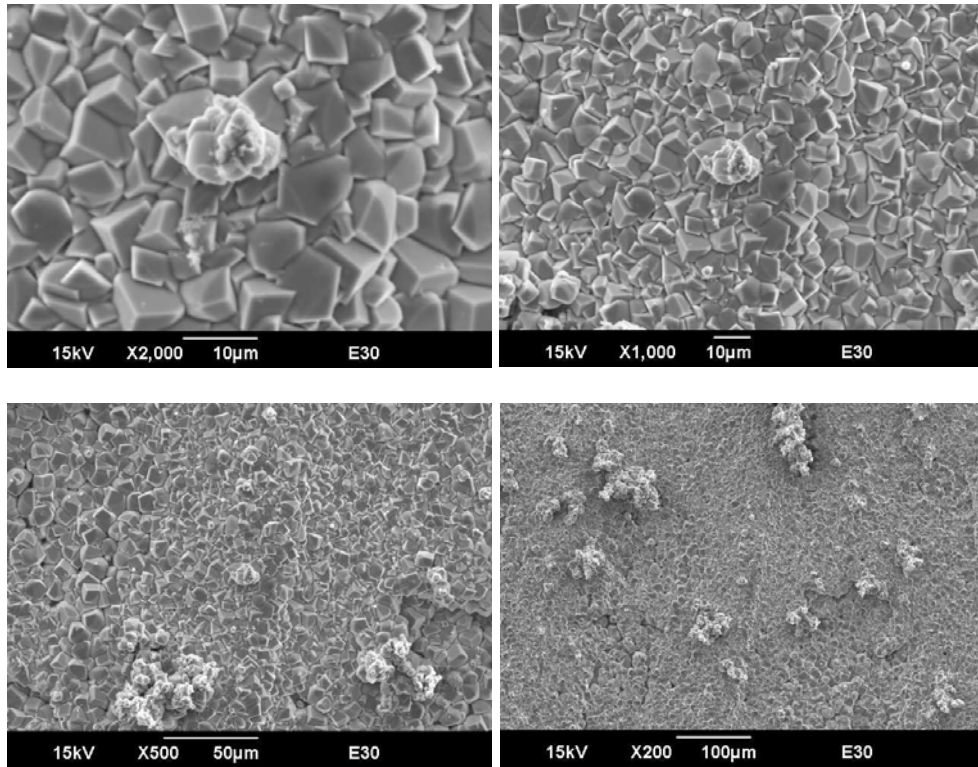


Figure 7 Iron carbonate film covered surface before contact angle test

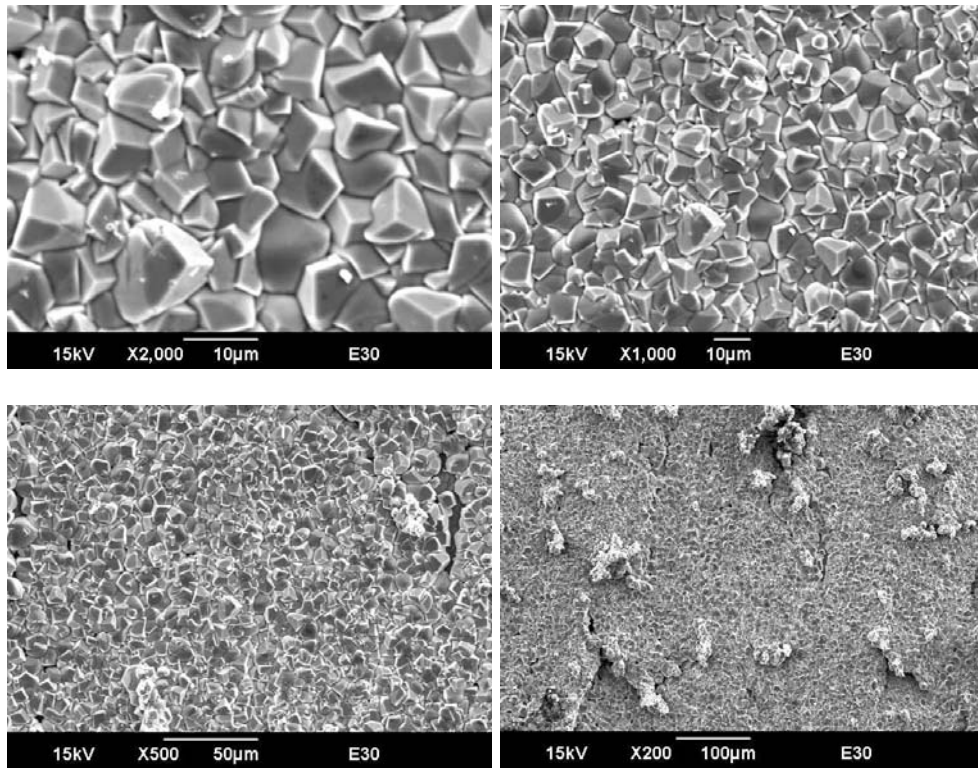


Figure 8 Iron carbonate film covered surface after contact angle test

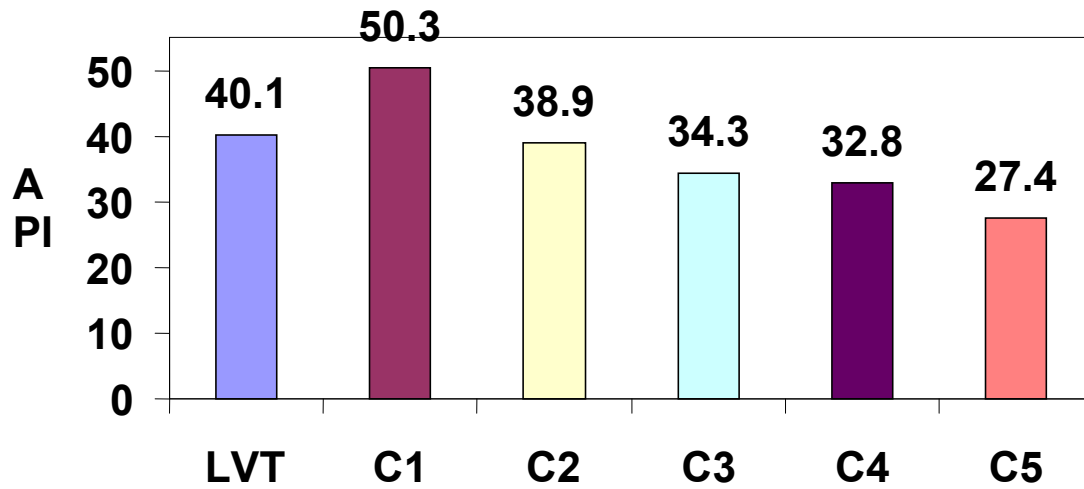


Figure 9 API value of oils¹²

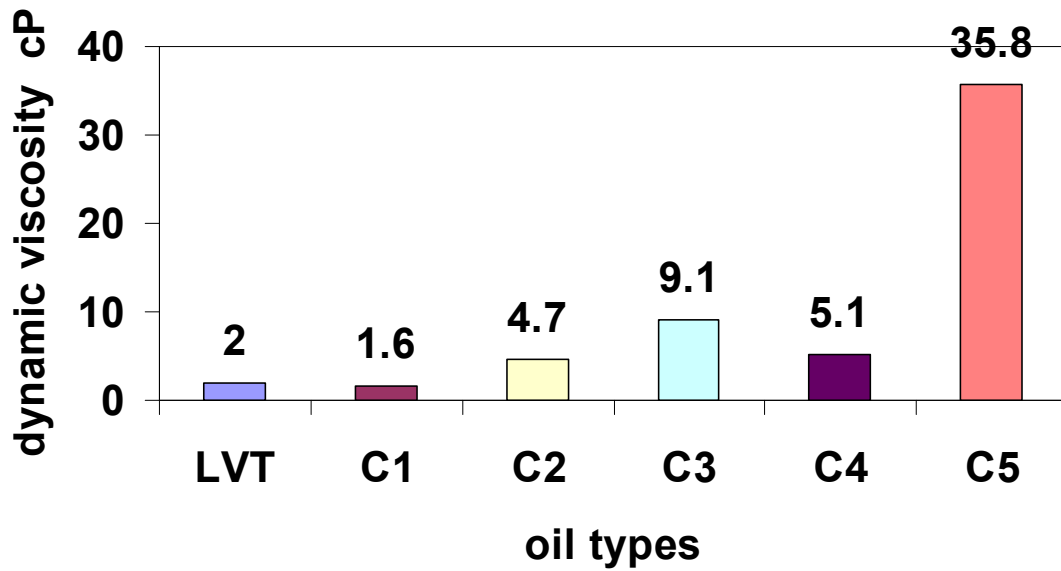


Figure 10 Dynamic viscosity of oils at 25°C¹²

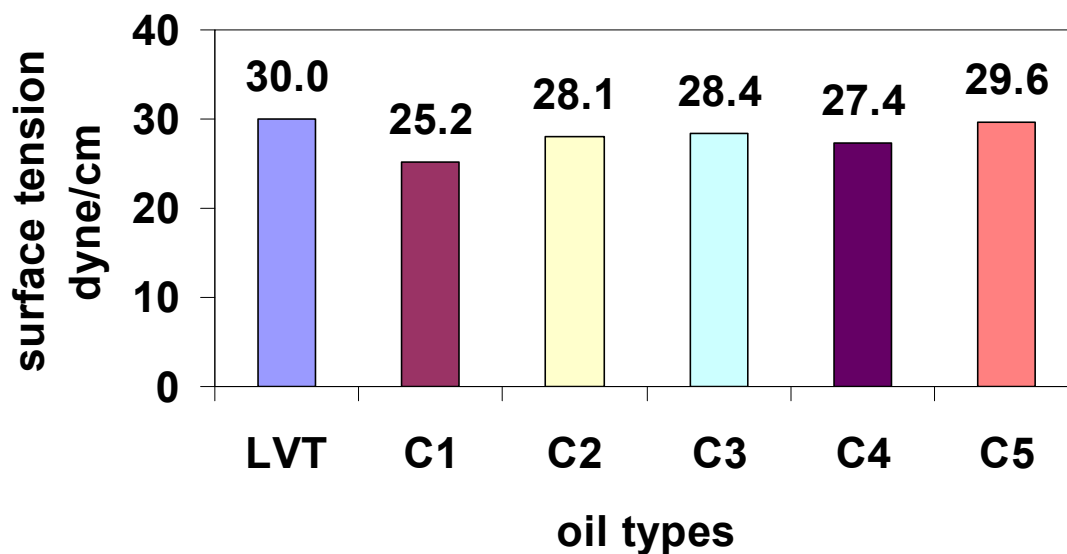


Figure 11 Surface tension of oils at 25°C¹²

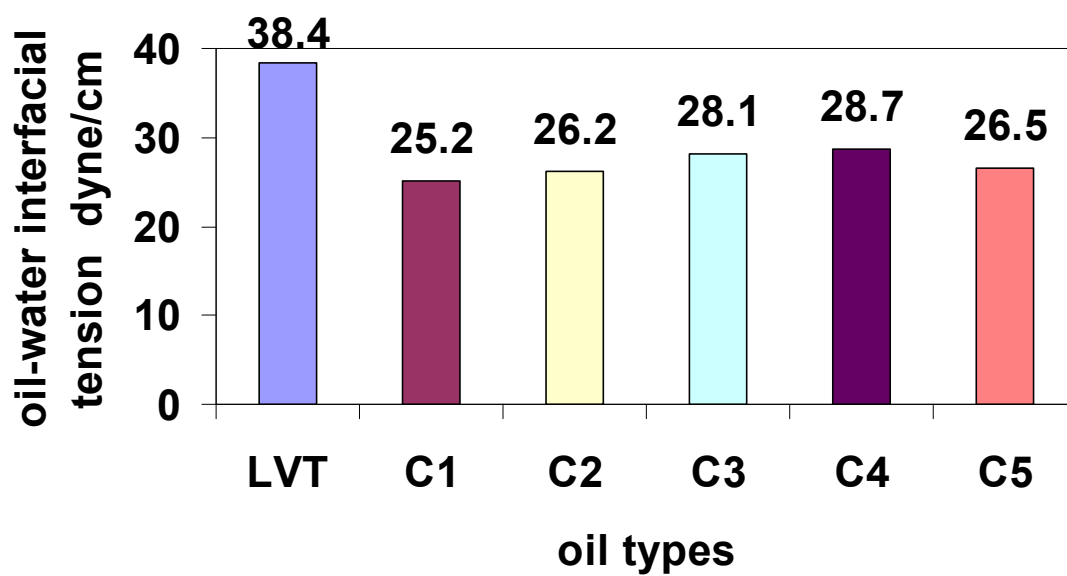


Figure 12 Oil-water interfacial tension of oils at 25 °C¹²

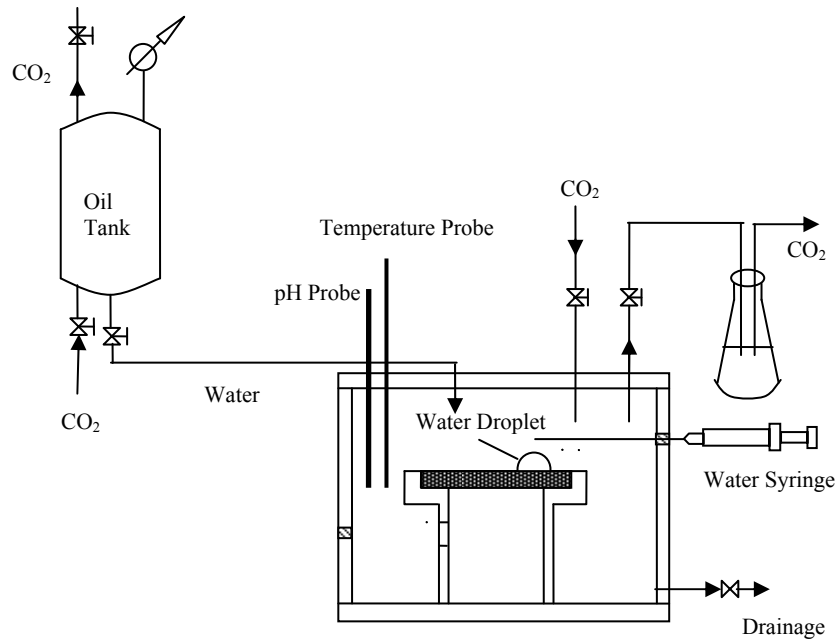


Figure 13 Schematic of experimental setup for water-in-oil droplet contact angle with metal surface

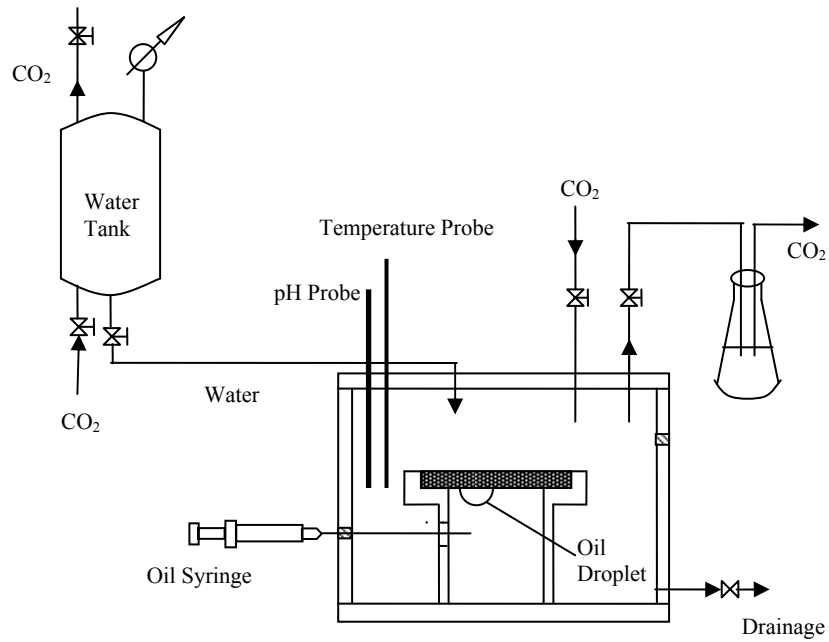


Figure 14 Schematic of experimental setup for water-in-oil droplet contact angle with metal surface

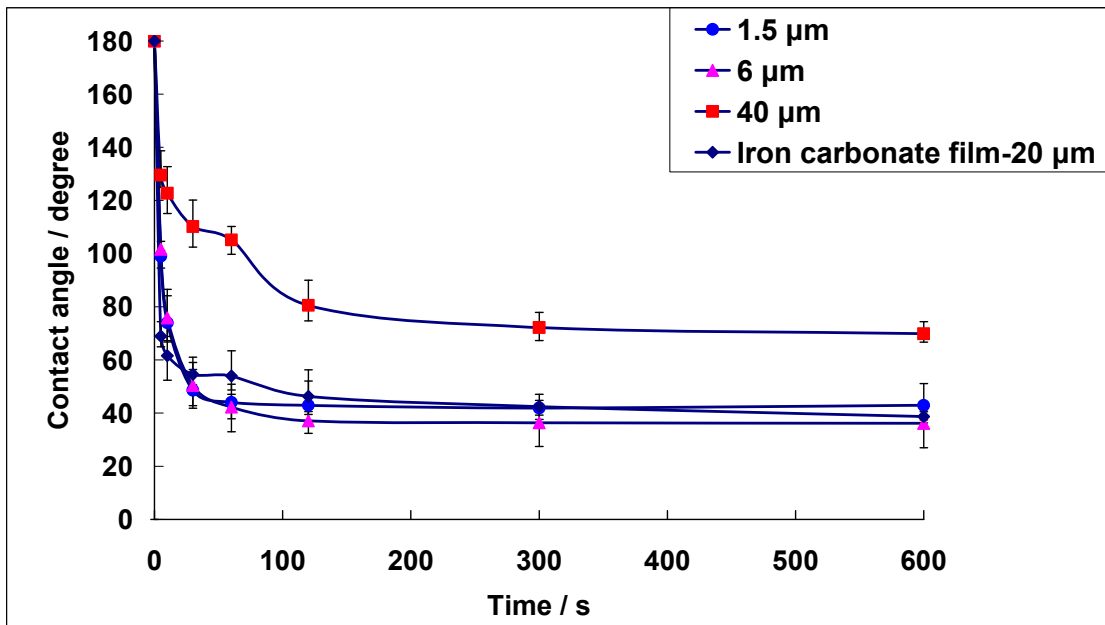


Figure 15 Water-in-oil contact angle on different steel surfaces versus time (600s)

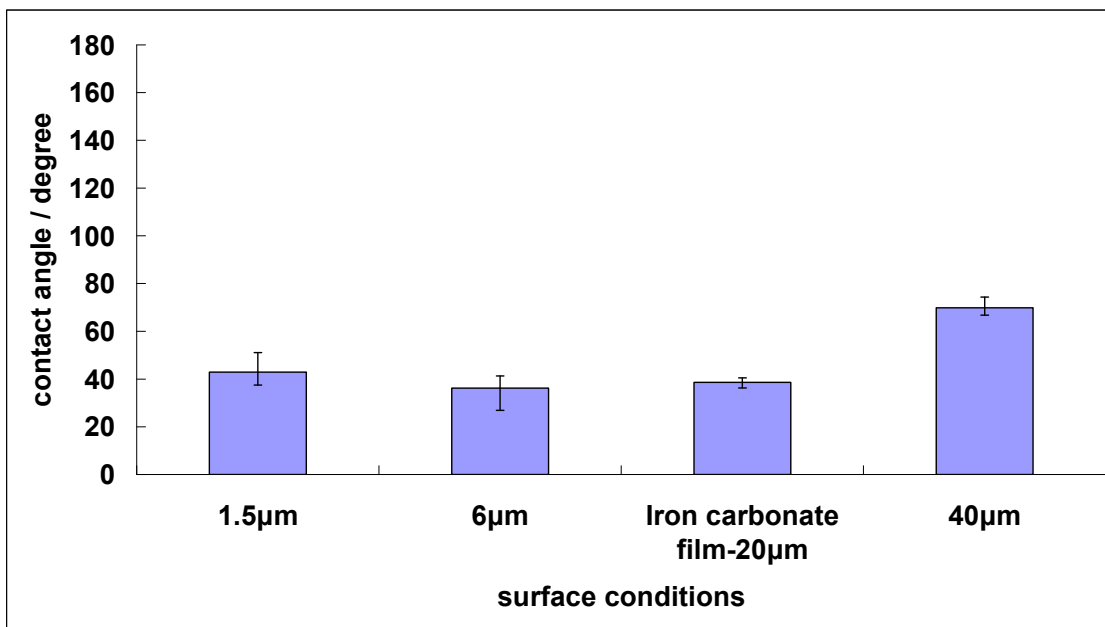


Figure 16 Equilibrium water-in-oil contact angle on different steel surfaces

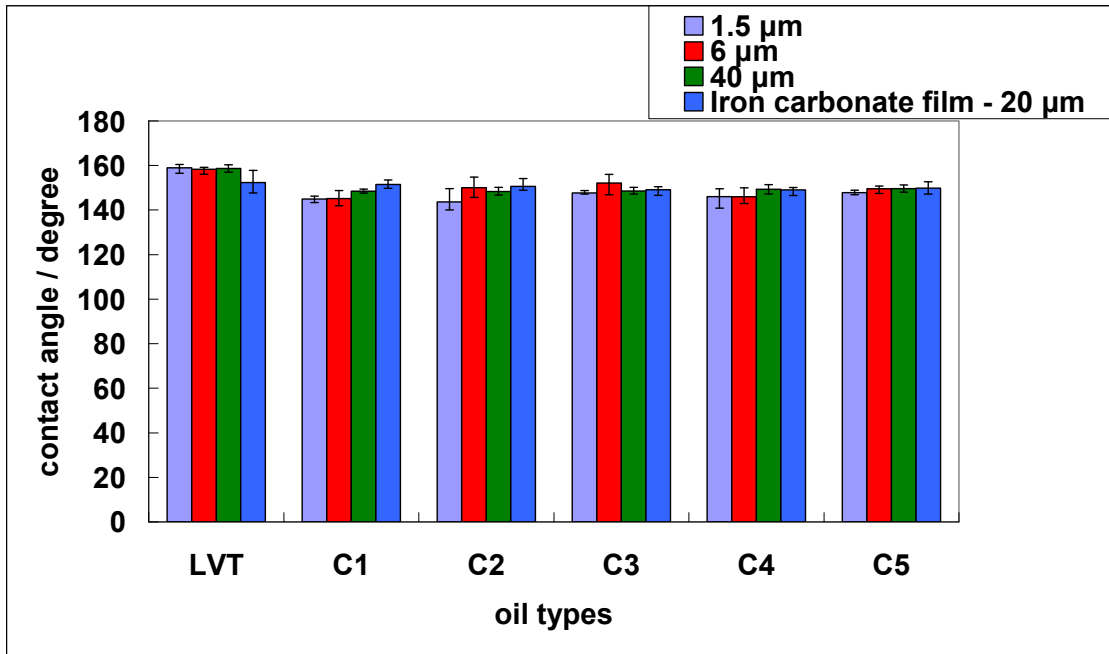


Figure 17 Equilibrium oil-in-water contact angle on different steel surface for different oils

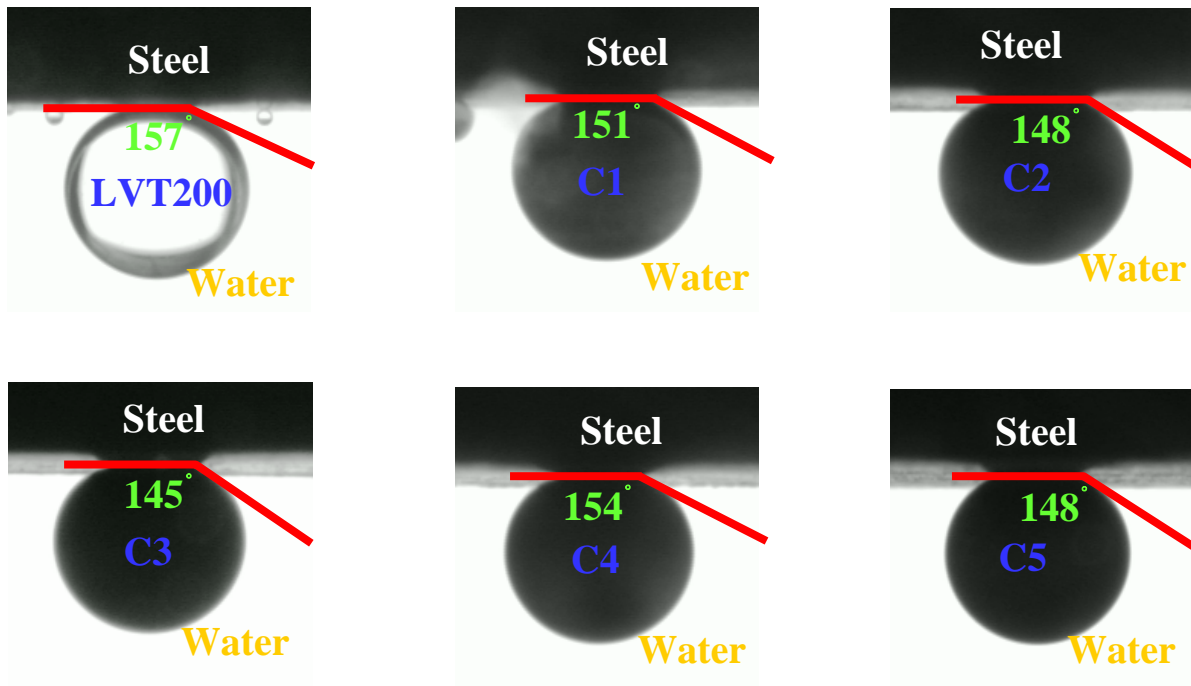


Figure 18 Typical images of different oil droplets on 6μm steel surface

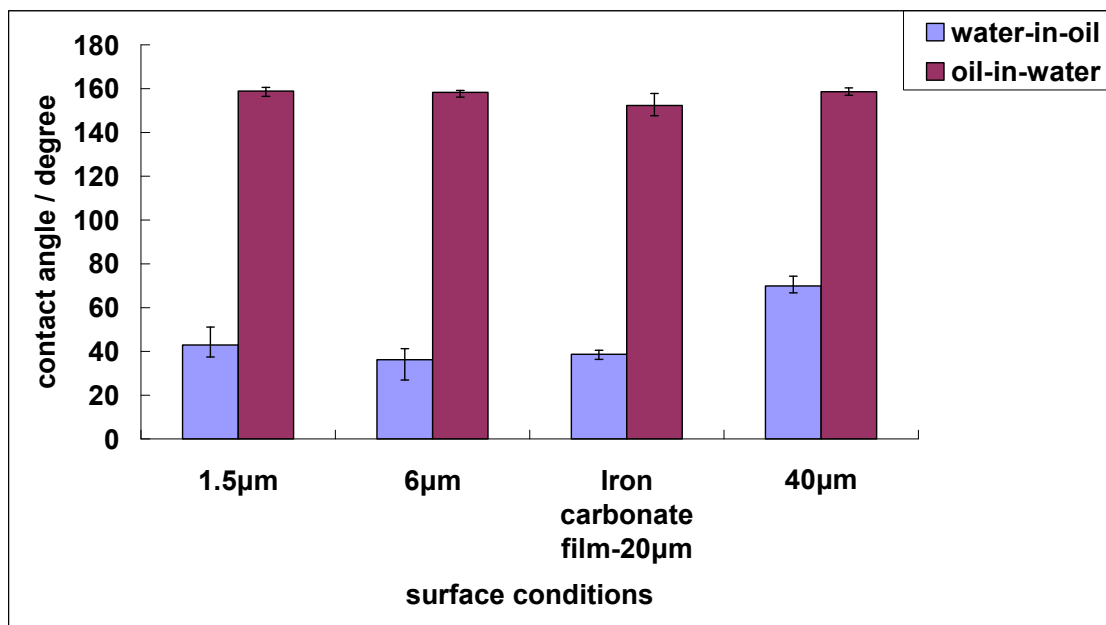


Figure 19 Equilibrium water-in-oil contact angle and oil-in-water contact angle with different steel surfaces for 1 wt% NaCl brine and LVT200